



Microbial and Transcriptomic Profiling Reveals Diet-Related Alterations of Metabolism in Metabolic Disordered Mice

Weize Zhu^{1†}, Ying Hong^{1†}, Yue Li², Yan Li¹, Jing Zhong^{1,3}, Xiaofang He¹, Ningning Zheng¹, Lili Sheng^{1*} and Houkai Li^{1*}

¹ School of Pharmacy, Shanghai University of Traditional Chinese Medicine, Shanghai, China, ² Department of Endocrinology, Shanghai Fifth People's Hospital, Shanghai Medical School, Fudan University, Shanghai, China, ³ Huzhou Key Laboratory of Molecular Medicine, Huzhou Central Hospital, Huzhou, China

OPEN ACCESS

Edited by:

Balamurugan Ramadass,
All India Institute of Medical Sciences
Bhubaneswar, India

Reviewed by:

Prasant Kumar Jena,
Cedars Sinai Medical Center,
United States
Priyadarshini Mishra,
All India Institute of Medical Sciences
Bhubaneswar, India

*Correspondence:

Houkai Li
hk_li@shutcm.edu.cn
Lili Sheng
fine919@163.com

[†]These authors have contributed
equally to this work

Specialty section:

This article was submitted to
Nutrition and Microbes,
a section of the journal
Frontiers in Nutrition

Received: 20 April 2022

Accepted: 30 May 2022

Published: 19 July 2022

Citation:

Zhu W, Hong Y, Li Y, Li Y, Zhong J,
He X, Zheng N, Sheng L and Li H
(2022) Microbial and Transcriptomic
Profiling Reveals Diet-Related
Alterations of Metabolism in Metabolic
Disordered Mice.
Front. Nutr. 9:923377.
doi: 10.3389/fnut.2022.923377

Metabolic disorders are the prelude of metabolic diseases, which are mainly due to the high-energy intake and genetic contribution. High-fat diet (HFD) or high-sucrose diet is widely used for inducing metabolic disorders characterized by increased body weight, insulin resistance, hepatic steatosis, and alteration of gut microbiome. However, the triangle relationship among diets, gut microbiome, and host metabolism is poorly understood. In our study, we investigated the dynamic changes in gut microbiota, and host metabolism in mice that were fed with either chow diet, HFD, or chow diet with 30% sucrose in drinking water (HSD) for continued 12 weeks. The gut microbiota was analyzed with 16S rDNA sequencing on feces. Hepatic gene expression profile was tested with transcriptomics analysis on liver tissue. The host metabolism was evaluated by measuring body weight, insulin sensitivity, serum lipids, and expression of proteins involved in lipid metabolism of liver. The results showed that HFD feeding affected body weight, insulin resistance, and hepatic steatosis more significantly than HSD feeding. 16S rRNA gene sequencing showed that HFD rapidly and steadily suppressed species richness, altered microbiota structure and function, and increased the abundance of bacteria responsible for fatty acid metabolism and inflammatory signaling. In contrast, HSD had minor impact on the overall bacteria structure or function but activated microbial bile acid biosynthesis. Fecal microbiota transplantation suggested that some metabolic changes induced by HFD or HSD feeding were transferrable, especially in the weight of white adipose tissue and hepatic triglyceride level that were consistent with the phenotypes in donor mice. Moreover, transcriptomic results showed that HFD feeding significantly inhibited fatty acid degradation and increase inflammation, while HSD increased hepatic *de novo* lipogenesis and inhibited primary bile acid synthesis alternative pathway. In general, our study revealed the dynamic and diversified impacts of HFD and HSD on gut microbiota and host metabolism.

Keywords: metabolic syndrome, high-energy diet, gut microbiota, metabolism, transcriptomic profiling

INTRODUCTION

Metabolic disorder mainly includes dysregulation of glucose and lipid metabolism, insulin resistance, and inflammation, which is predominantly due to the excessive energy intake, in addition to genetic susceptibility (1, 2). Metabolic disorder is the prelude of metabolic diseases consisting of obesity, non-alcoholic fatty liver disease (NAFLD), type 2 diabetes (T2DM), hyperlipidemia, and metabolic syndrome (3–5). It is well known that the prevalence of Western diet is the key factor contributing to the development of metabolic disorders (6–9).

The commensal gut microbiome is regarded as a “metabolic organ” for host (10), which not only takes part in intestinal nutrients absorption (11, 12), but also regulates host metabolism by producing microbial metabolites like short-chain fatty acids (acetate, propionate, butyrate, etc.) (13–15), or secreting peptides like GLP-1 modulating glucose homeostasis (16). On the contrary, bacteria-derived lipopolysaccharide (LPS) induces metabolic endotoxemia resulting to development of metabolic diseases (17–21). Increasing evidence has demonstrated the involvement of gut microbiome in metabolic diseases, which are characterized by dramatic changes in gut microbiota in both structure and function (22, 23). Although the causative roles of gut microbiome in metabolic diseases have been well-evidenced, the exact relationship among gut microbiome, diets, and metabolic disorders is still elusive.

High-energy diets are widely used in experimental studies to induce animal models with metabolic disorders, including high-fat diet (HFD) and/or high-sugar (sucrose/ fructose/glucose) diet (HSD) (24–26). The diet-induced animal models with metabolic disorders are not only characterized by typical phenotypes that are present in human patients (26, 27), but also show dramatic changes in gut microbiome (28, 29). Yang et al. (30) reported the significant increases in pathogenic bacteria *Alistipessp.Marseille-P5997* and *Alistipessp.5CPEGH6* while reduced abundance of *Parabacteroides distasonis* in HFD-fed mice, accompanied by impaired gut barrier function. Wang et al. (31) found that HFD-fed mice showed significantly altered *Blautia*, *Desulfovibrio*, and *Lachnospiraceae_NK4A136_group* abundance, whereas decreased abundance of *Desulfovibrio vulgaris* was also observed in HFD-fed mice, and supplement of *Desulfovibrio vulgaris* improved HFD-induced hepatic steatosis (32). Meanwhile, the impacts on gut microbiota and gut permeability were investigated in mice that were fed with high glucose or fructose diets, which showed that high glucose or fructose feeding resulted in poor gut microbial diversity, characterized by a lower proportion of Bacteroidetes and increased Proteobacteria, as well as altered expression of tight junction proteins (33). As a result, although the dietary impacts on gut microbiota were well-established (34–36), the exact relationship between diet-induced alteration of gut microbiota and host metabolism remains unclear.

In this study, we systemically evaluated the dynamic impacts of a 12-week HFD and high-sucrose feeding on gut microbiota and host metabolism in mice by measuring the body weight gain, serum lipids, hepatic steatosis, glucose tolerance and insulin sensitivity, composition of gut microbiota, and hepatic gene expression profiles. Our results showed that HFD feeding

TABLE 1 | Caloric information of diet.

Caloric information	Chow diet	High-sucrose diet	High-fat diet
Protein:	22.8% Kcal	22.8% Kcal	20.0% Kcal
Fat:	13.8% Kcal	13.8% Kcal	60.0% Kcal
Carbohydrate:	63.4% Kcal	63.4% Kcal	20.0% Kcal
Energy density in diet:	3.65 Kcal/g	3.65 Kcal/g	5.21 Kcal/g
Energy density in drinking water:	0.00 Kcal/ml	1.31 Kcal/ml	0.00 Kcal/ml

induced more significant changes in insulin resistance, hepatic steatosis, gut microbiota, and gene expression profile of liver than HSD feeding in the context of comparable amount of energy intake. Moreover, the gut microbiota from HFD and HSD feeding mice induced different impacts on metabolism. Taken together, our results revealed the dynamic and diversified impacts of HFD and HSD feeding on gut microbiota and host metabolism.

MATERIALS AND METHODS

Mice

All animals were purchased from Shanghai SLAC Laboratory Animal Co., Ltd and bred at the experimental animal center, Shanghai University of Traditional Chinese Medicine. They were housed in a regulated barrier system facility at 23–24°C with 60 ± 10% relative humidity and a 12:12-h light/dark cycle under specific-pathogen-free (SPF) grade. All experimental procedures were approved by the Animal Experiment Institution of Shanghai University of Traditional Chinese Medicine.

Time-Course Animal Experiment

After 1-week accommodation, 105 4-week-old male C57BL/6 mice were randomly divided into three groups and were fed with chow diet and normal drinking water (Con, $n = 30$), chow diet and 30% sucrose in drinking water (HSD, $n = 30$, #V900116, Merck, Germany), or high-fat diet and normal drinking water (HFD, $n = 45$, 60% fat, #D12492, Research Diet, USA, **Table 1**). Ten mice from Con and HSD groups or 15 mice from HFD group were killed with 1% pentobarbital sodium solution intraperitoneally at the 4th, 8th, and 12th week, respectively. Tissue samples were collected, weighted, and immediately frozen in liquid nitrogen and stored at -80°C for further analysis. Part of liver tissue and epididymal fat tissue were fixed with 10% neutral formalin for subsequent HE staining. Tissue index = tissue weight (g)/ body weight (g).

Fecal Microbiota Transplantation Animal Experiment

In the FMT experiment, 4-week-old male C57BL/6 mice were divided into five groups: Con, R-HSD, R-HFD, D-HSD, and D-HFD. Con group were fed with chow diet and normal drinking water (Con, $n = 6$). D-HSD were fed with chow diet and 30% sucrose in drinking water (D-HSD, $n = 6$), and D-HFD were fed with high-fat diet and normal drinking water (D-HFD, $n = 6$) during the entire experiment. After 4 weeks of HSD or

HFD feeding, fresh fecal sample was continuously collected while study continued and fed to recipient groups. R-HSD and R-HFD groups were fed with chow diet and normal drinking water and received antibiotics for 1 week before FMT to deplete the gut microbiota (oral gavage of 10 g/L Metronidazole, 5 g/L Vancomycin, and 10 g/L Neomycin at the dose of 0.1 mL/10 g body weight, 1 g/L Ampicillin in drinking water, $n = 6$ per group). Oral gavage of the bacterial suspension from D-HSD or D-HFD groups started from Week 4 and continued for 4 weeks. The bacterial suspension procedure is as follows: Freshly collected feces were diluted in PBS at a ratio of 50 mg feces/ml PBS, homogenized, and filtered with a germfree sieve (0.2 mm, Thermo, USA), and the R-HSD and R-HFD group mice were administered 200 μ l of the fecal suspension by oral gavage once every day for 4 weeks.

Histological Evaluation on the Degree of Hepatic Steatosis

Liver tissues were fixed with 10% formalin for 24 h, embedded in paraffin, and then stained with hematoxylin–eosin staining (H&E) using a standard protocol. Hematoxylin staining was used for nuclear counterstaining (blue), and eosin was used to stain the cytoplasm red. The degree of hepatic steatosis was evaluated according to previous publication in a blinded way (37). The criteria for scoring include grade 0, no steatosis; grade 1, steatosis involved <25%; grade 2, steatosis involved between 26 and 50 %; grade 3, steatosis involved between 51 and 75 %; and grade 4, steatosis involved >75%.

Serum Biochemistry Index Test

Mice were fasted for 12 h, and blood sample was collected before mice been killed, left undisturbed at room temperature for 1 h, and then centrifugated at 4°C, 4,000 rpm for 10 min to separate serum. Serum TC (#A111-1-1, Nanjing Jiancheng, China), TG (#A110-1-1, Nanjing Jiancheng, China), HDL-C (#A112-1-1, Nanjing Jiancheng, China), LDL-C (#A113-1-1, Nanjing Jiancheng, China), ALT (#C009-2-1, Nanjing Jiancheng, China), NEFA (#A042-2-1, Nanjing Jiancheng, China), and insulin (#EZRMI-13K, Merck, Germany) were tested according to the instruction manual.

Liver Triglycerides Examination

Hepatic lipids were extracted according to the optimized Folch method (38). Briefly, 12.5 mg of liver tissue was homogenized in 500 μ l of chloroform: methanol (2:1, v: v) and centrifuged briefly. Then, tissues were grinded at 60 Hz for 1 min, vortexed for 1 min, and centrifugated at 4°C, 4,000 rpm for 10 min. About 10 μ l (60 μ l for TC test) supernatant was collected and dried at room temperature. The residue was resuspended with 10 μ l ultra-pure water, and the TG and TC levels were measured with the instruction manual.

Glucose Tolerance Test and Insulin Tolerance Test

GTT was conducted in mice after overnight fasting. Then, mice were injected intraperitoneally with 10% (g/v) glucose solution at a dosage of 1 g/kg body weight, and then, blood

glucose levels were measured using glucose meter (ACCU-CHEK Performa, Germany) at 0, 15th, 30th, 60th, 90th, and 120th min. ITT was performed in fed mice in which all of the mice were intraperitoneally injected with human insulin (0.75 units/kg body weight, Novo Nordisk) according to previous test, and then, blood glucose levels were measured essentially as earlier described.

16S rRNA Gene Sequencing and Analysis

The genomic DNA extraction and the processing and quality control of raw sequencing data were performed according to the previous study (32). Briefly, the genomic DNA was extracted by QIAamp DNA Mini Kit (#51304, QIAGEN, Germany). Then, the qualified DNA samples were amplified by universal primers of 16S rDNA V3–V4 region (338F and 806R) (39) and sequenced by Illumina MiSeq PE300 system (Illumina, USA). After pretreatment by Fastp (40) and FLASH (41), sequences were divided into operational taxonomic units (OTUs) which have high similarity ($\geq 97\%$) by UPARSE (42) and removed chimeric sequences by UCHIME (43) based on Silva 16S rRNA database (SSU123) (44). The taxonomy of each sequence was analyzed by RDP classifier algorithm (45) with confidence threshold of 70%. Alpha diversity of each sample was assessed by Mothur (46), including Chao, Ace, and Sob index for bacterial richness analysis, with Simpson and Shannon index for bacterial richness and evenness analysis. The principal coordinate analysis (PCoA) was conducted to reflect community similarity of gut microbiota in each group, distance algorithm was weighted by UniFrac (47), and PERMANOVA analyses assessed by QIIME (48) were conducted to evaluate the significant differences among groups. Relative abundances were calculated by dividing the absolute abundances per phylum, family, or genus by the total sequence count per sample. To predict potential microbial functional, OTUs from each microbial sample were predicted using the PICRUST (49). The Spearman rank coefficient was used to assess correlations between genus level and phenotypes.

Transcriptomics Array

The RNA extraction and the processing and quality control of raw sequencing data were performed according to the previous study (32). Briefly, total RNA was extracted by TRIzol (#15596018, Invitrogen, USA), and quality was determined. Then, established RNA library, reverse synthesize cDNA by kits, and the cDNA, as a probe, were immobilized on the chip, labeled with fluorescent molecules, and then hybridized with the chip, and the changes in gene expression levels can be detected by analyzing the fluorescence intensity of the hybridization of the probe. The principal component analysis (PCA) was performed to compare gene similarities of hepatic tissues in each group. KEGG pathway enrichment analysis was performed by the DAVID Bioinformatics Database (<http://david.abcc.ncifcrf.gov/>).

Statistical Analysis

Data are shown as means \pm s.e.m unless otherwise noted. Statistical significance of body weight and biochemistry index was determined with the unpaired two-tailed Student's *t*-test. The statistical significance of hepatic steatosis scores was evaluated

with non-parametric Kruskal–Wallis test followed by the Mann–Whitney *U*-test. $P < 0.05$ was considered statistically significant.

RESULTS

High-Fat Diet and High-Sucrose Intake Caused Divergent Changes in Metabolism in Mice

To test the effect of different high-energy diets on the overall metabolism, a series of indicators of metabolic disorder was measured in high-fat and high-sucrose diet-fed mice with different intervention durations. Mice were fed with chow diet, high-fat diet (HFD, 60% fat), or high-sucrose diet (HSD, 30% sucrose in water) for 4, 8, and 12 weeks. First, both HFD and HSD led to time-dependent increases in body weight over 12 weeks with higher body weight in HFD-fed mice, though both groups had the same energy intake (Figures 1A,B). The weight and ratio of white adipose tissue (WAT), brown adipose tissue (BAT), and liver were significantly increased in HFD and HSD-fed mice, with higher WAT and BAT weight with ratio in HSD group after 12-week intervention (Figures 1A,C). Both diets elevated serum lipid. However, serum triglycerides (TG) were much higher in HSD-fed mice than HFD-fed mice at all three studied time point, while non-esterified fatty acid (NEFA) was higher in HSD-fed mice than HFD-fed mice after 12-week intervention (Figures 1D,E). In contrast, serum high-density lipoprotein cholesterol (HDL-C), low-density lipoprotein cholesterol (LDL-C), and total cholesterol (TC) were higher in HFD group than HSD group at all-time points (Figures 1F–I). In addition, HFD induced more severe fat accumulation in the liver, which was revealed by higher hepatic steatosis grade and liver TG (Figures 1H,J). Moreover, serum alanine aminotransferase (ALT) was only elevated in HFD group (Figure 1K). These findings suggested that both HFD and HSD can cause metabolic disorders with different extends, and compared to HSD, HFD has a more significant effect on inducing fatty liver and liver injury.

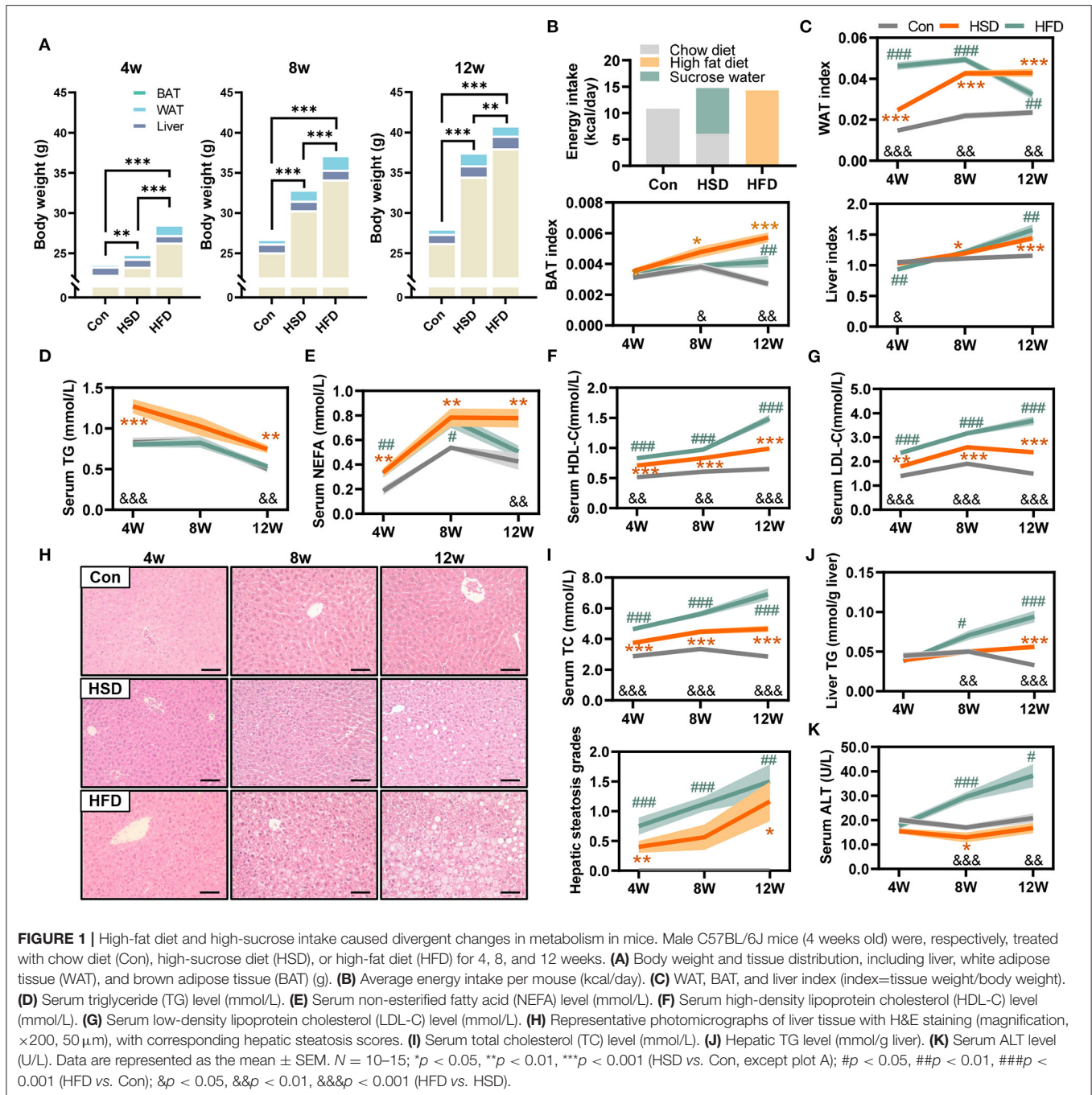
To further explore the effect of different dietary intakes on glucose metabolism, we conducted glucose tolerance tests (GTT) and insulin tolerance tests (ITT) after 4-, 8-, and 12-week intervention. The result showed HFD induced more severe glucose intolerance than HSD. HFD induced glucose intolerance as early as 4 weeks, while HSD started to induce glucose intolerance only after 8 weeks (Figure 2A). The results of ITT test also show that the decrease in insulin sensitivity occurs after 12-week intervention in both HFD and HSD groups (Figure 2B). Meanwhile, we found HFD, but not HSD, could significantly increase fasting blood glucose level, fasting serum insulin level, and HOMA-IR (Figure 2C). These results indicated that HFD and HSD could both induce glucose metabolism disorder, with more severe degree and earlier in HFD group than HSD group.

High-Fat Diet, but Not High-Sucrose Intake Resulted in Dramatic Alteration of Gut Microbiome

Extensive research has shown that gut dysbiosis is a central initiator of obesity-related diseases including NAFLD, type 2

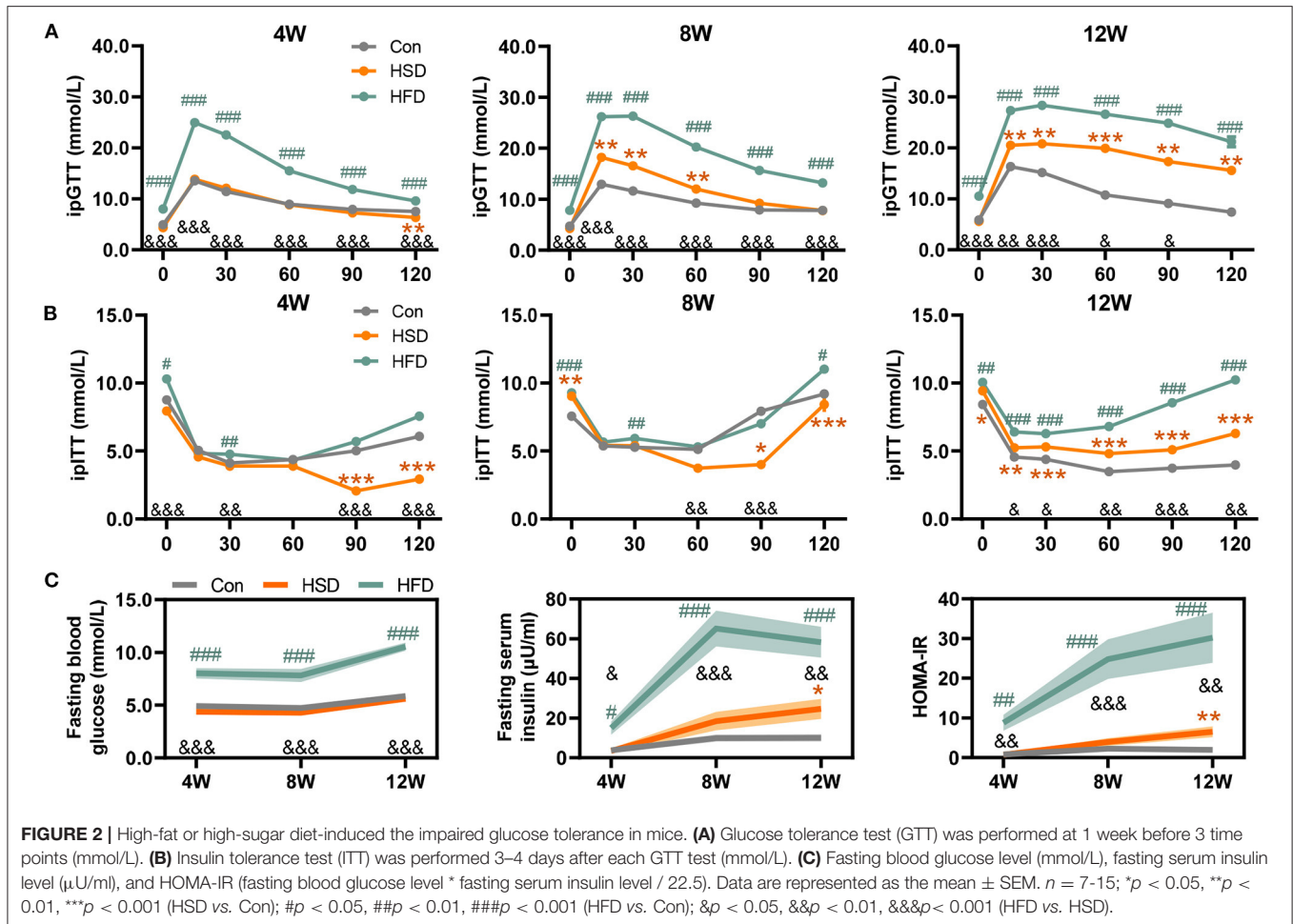
diabetes, and metabolic syndrome (50, 51). Here, we compared the effects of HFD or HSD on the community structures of the gut flora after 4-, 8-, and 12-week dietary intervention. The compositional alteration of gut microbiota was evaluated based on 16S rRNA gene sequencing. An average of $37,740 \pm 504$ valid reads was obtained that covered the majority of bacterial diversity. We found that HFD reduced bacterial richness (including Sobs, Chao, and Ace indexes) and Simpson index, with no significant difference in Shannon index at all-time points. However, HSD did not affect bacterial richness and evenness, with the change in Simpson index to a small extent (Figure 3A). The weighted UniFrac principal coordinate analysis (PCoA) also showed that HFD groups were significantly separated from Con and HSD groups on PCoA1, with no separation on Con and HSD groups (Figure 3B). In addition, at the phylum level, HFD increased the relative abundance of Firmicutes and Proteobacteria, but reduced Bacteroidetes, leading to the increase in Firmicutes/Bacteroidetes (F/B) ratio compared to the Con group, with no variation detected between HSD and Con groups (Figure 3C). Interestingly, although the relative abundance of Proteobacteria was elevated in HFD, it was decreased with the increase of intervention time (Figure 3C). We also analyzed the top 10 families which covered 96.09% of total bacteria. Most families showed significant change in HFD group. For instance, HFD increased the abundance of Ruminococcaceae, Bacteroidaceae, Rikenellaceae, Helicobacteraceae, Desulfovibrionaceae, and Porphyromonadaceae, but reduced the abundance of Bacteroidales_S24-7 group, Lachnospiraceae, Prevotellaceae, and Verrucomicrobiaceae (Figure 3D). HSD altered the relative abundance of several family level, with reduced Verrucomicrobiaceae and increased Prevotellaceae and Bacteroidaceae at 4 weeks, as well as reduced Ruminococcaceae and increased Porphyromonadaceae at 12 weeks (Figure 3D). At genus level, HFD increased the abundance of *Ruminiclostridium_9*, *Blautia*, *Desulfovibrio*, *Oscillibacter*, *Alistipes*, *Ruminiclostridium*, and *Bacteroides*, but reduced the abundance of *Lachnospiraceae_NK4A136_group*, *Alloprevotella*, and *Akkermansia*, which aligned with the family-level distinction. Differ from HFD group, HSD increased *Alloprevotella* at 4 and 8 weeks and reduced the abundance of *Ruminiclostridium_9* and *Oscillibacter*, leading to the opposite trend on Ruminococcaceae and Prevotellaceae compare with HFD (Figure 3E).

To assess whether gut microbiota alterations influenced gut microbiota function, PICRUSt2 analysis was performed for functional profile predictions of microbiota based on 16S rRNA gene. We found that the huge impact of HFD on microbiota structure was also accompanied by significant changes in microbial function. Compared with the Con group, HFD-induced bacterial functional changes in KEGG level 2 mainly involved in reduced biosynthesis of secondary metabolites, other amino acids metabolism, nucleotide metabolism, lipid metabolism, endocrine system, and increased amino acid metabolism, immune system, and signal transduction. In contrast, HSD regulated bacterial function only at early stage (Figure 4A). When comparing the effect of HFD with HSD,



HFD activated xenobiotic biodegradation and metabolism, amino acid metabolism, immune system signal transduction, and excretory system, while HSD activated carbohydrate metabolism, biosynthesis of other secondary metabolites, metabolism of other amino acids, nucleotide metabolism, and lipid metabolism in most cases. Further functional characterization of the above pathway at KEGG level 3 showed that HFD significant reduced bacterial glucose metabolism including starch and sucrose metabolism, fructose and mannose metabolism, and glycerophospholipid metabolism, with early

significant reduction in glucagon signaling and following significant increase in PI3K-Akt signaling. HFD also increased microbial fatty acid metabolism at early stage, including fatty acid biosynthesis and fatty acid degradation, and continuous increased inflammation-related signaling, including NOD-like receptor signaling pathway and toll and imd signaling pathway (Figure 4B). HSD activated microbial glucose metabolism and reduced insulin regulation signal only at early stage, but activated primary bile acid biosynthesis and secondary bile acid biosynthesis only at late stage (Figure 4B). The above findings



suggested that the impact of HFD on gut microbiota was more robust and sustained than HSD.

Diet-Dependent Specific Correlation Between Mouse Phenotypes and Gut Microbiota

To explore the relationship between phenotypes and gut microbiota, we performed Spearman's correlation based on different diets. When comparing HSD and Con groups, we noticed *Odoribacter* and *Coprococcus_1* were positively correlated with liver and WAT weight, as well as fasting insulin and serum NEFA level, while *Prevotellaceae_NK3B31_group* was negatively correlated with liver and WAT weight (Figure 5A). When comparing HFD and Con groups, *Odoribacter* and *Prevotellaceae_NK3B31_group* also correlated with most of these phenotypes, which is similar as we found in HSD vs. Con groups. However, more families were either positively or negatively with mouse phenotypes in HFD groups, suggesting HFD-induced dramatic changes in gut microbiota might account for diet-induced metabolic disorder (Figure 5B). Next, we further studied how different gut microbiota compositions in HSD and HFD groups are related to

mouse phenotypes. *Norank_f_Bacteroidales_S24-7_group* and *[Eubacterium]_coprostanoligenes_group*, the abundance of which were elevated in HFD than HSD group, were negatively associated with serum TC, LDL, ALT, and fasting glucose level. Some bacterial families that were increased in both HFD vs. Con and HFD vs. HSD groups, such as *Alistipes*, *Bilophila*, *Bacteroides*, *Mucispirillum*, *Ruminiclostridium*, *Ruminiclostridium_9*, *Oscillibacter*, and *Anaerotruncus*, were positively related to serum TC, LDL, ALT, HDL, as well as fasting insulin and glucose level in most cases (Figures 5C,D). These findings suggested that certain bacterial families shifted by HFD might account for the more severe metabolic disorders in HFD-fed mice.

High-Fat and High-Sucrose Diet-Induced Lipid Metabolic Dysregulation Is Gut Microbiota-Dependent

To test whether the phenotypic changes in HFD- and HSD-fed mice were due to the modulation of gut microbiota composition and function, a fecal microbiota transplantation (FMT) experiment was performed (Figure 6A). Though no statistical differences were observed in the body weight,

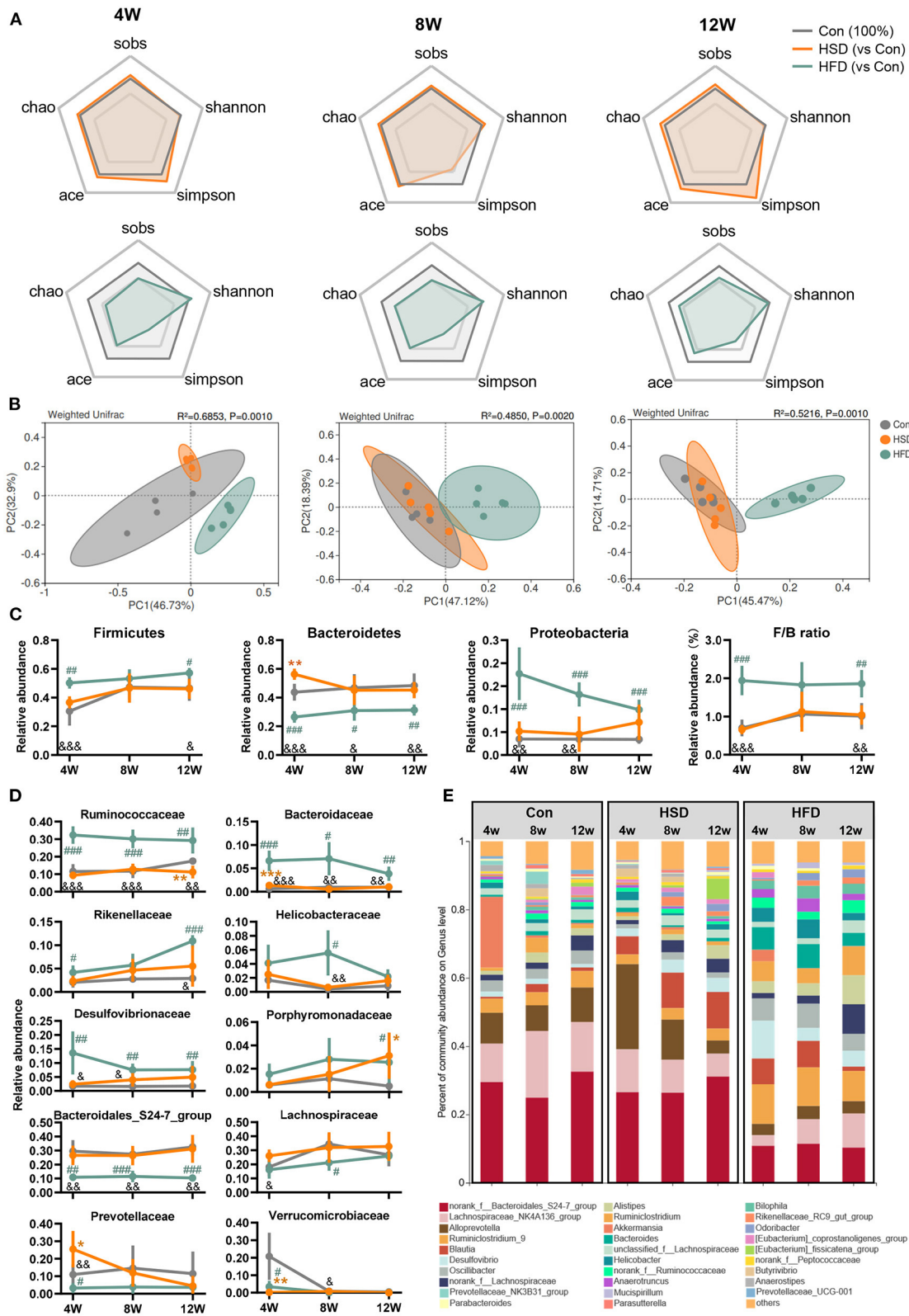


FIGURE 3 | High-fat diet, but not high-sucrose intake resulted in dramatic alteration of gut microbiome. Fecal samples of Con, HSD, and HFD groups at three time points were analyzed with 16S rRNA gene sequencing. **(A)** The relative change in α diversity index, including Sobs, Chao, Ace, Simpson, and Shannon index, *(Continued)*

FIGURE 3 | normalized with Con group (100%). **(B)** Weighted UniFrac based PCoA analysis among groups with permutational multivariate analysis of variance (PERMANOVA). **(C)** Relative abundance of bacteria at phylum level and Firmicutes/Bacteroidetes (F/B) ratio. **(D)** Relative abundance of top 10 abundant family. **(E)** Bacterial taxonomic profiling at genus level. Data are represented as the mean ± SEM. $n = 4-5$; * $p < 0.05$, ** $p < 0.01$, *** $p < 0.001$ (HSD vs. Con); # $p < 0.05$, ## $p < 0.01$, ### $p < 0.001$ (HFD vs. Con); & $p < 0.05$, && $p < 0.01$, &&& $p < 0.001$ (HFD vs. HSD).

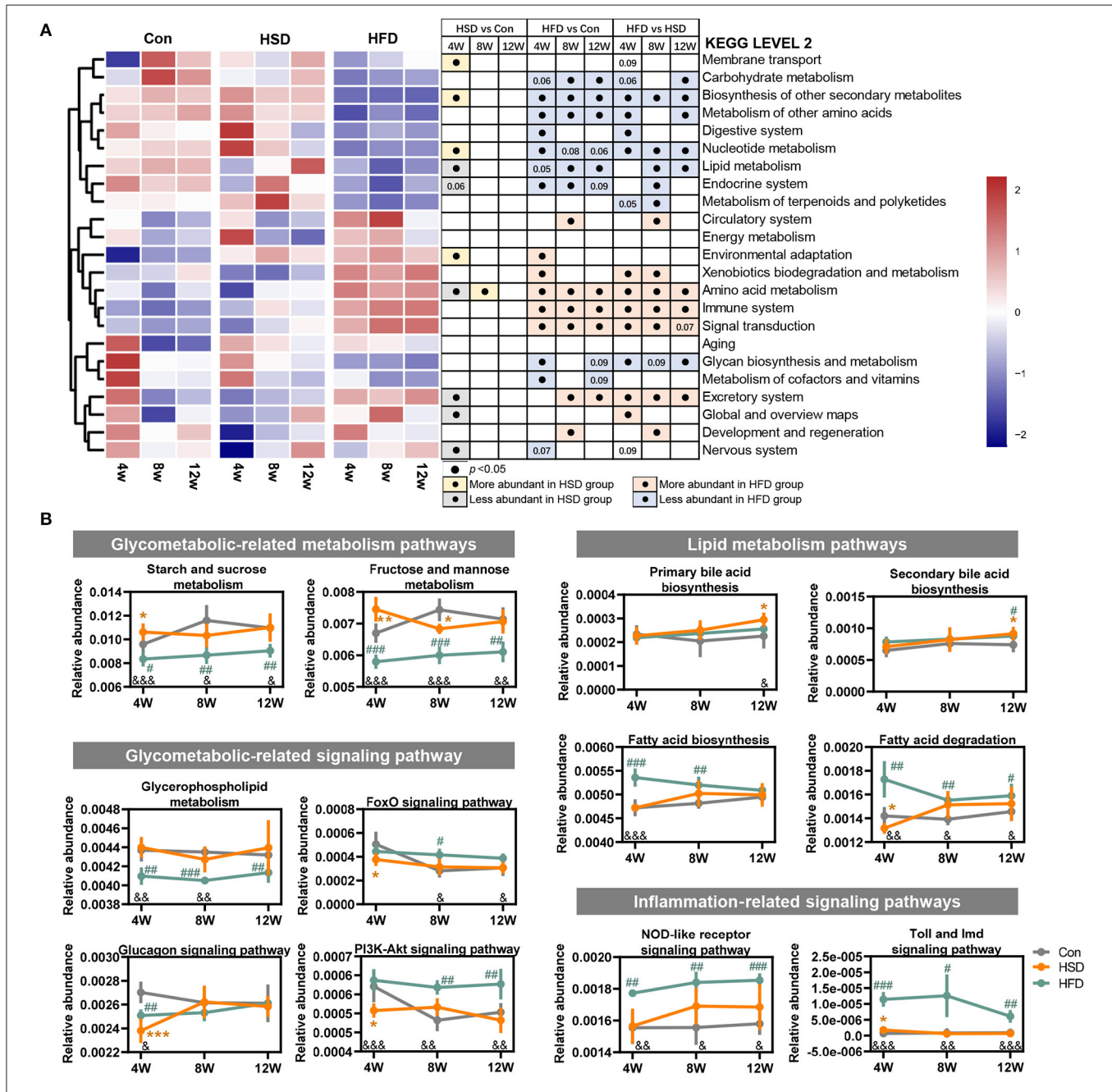


FIGURE 4 | High-fat diet changed the main functions of gut dysbiosis in mice. Microbial functions regulated by HFD or HSD were predicted with PICRUSt2. **(A)** Heatmap summarizing the changes in gut microbial community function at KEGG level 2, following Con, HSD, and HFD group at three time point in mice. Black circle represents the KEGG pathway which was significantly altered relative to Con or HSD groups at same time point ($p < 0.05$). **(B)** Relative abundance of the pathways related to glycolipid metabolism disorder. Data are represented as the mean ± SEM. $n = 4-5$; * $p < 0.05$, ** $p < 0.01$, *** $p < 0.001$ (HSD vs. Con); # $p < 0.05$, ## $p < 0.01$, ### $p < 0.001$ (HFD vs. Con); & $p < 0.05$, && $p < 0.01$, &&& $p < 0.001$ (HFD vs. HSD).

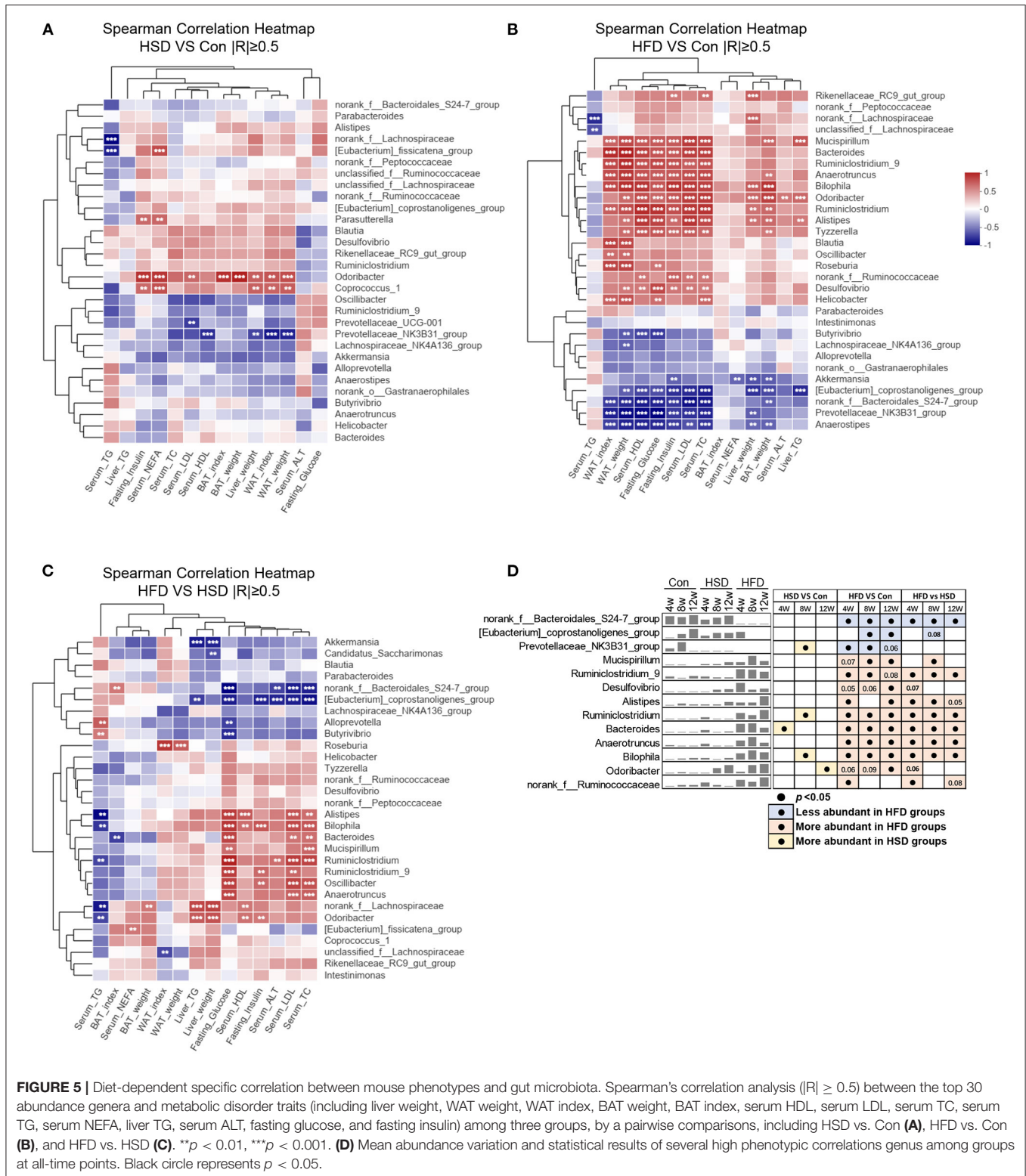
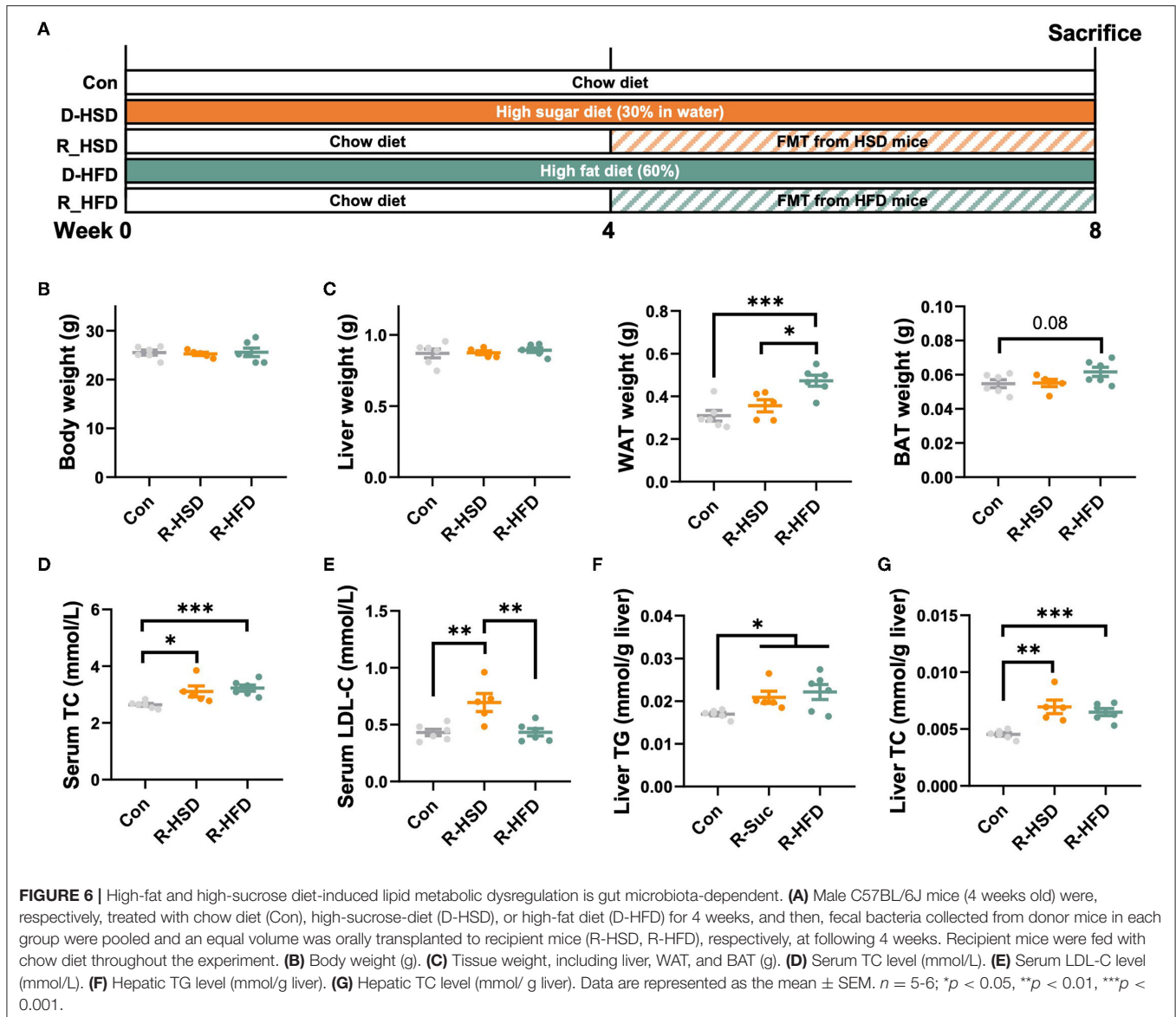


FIGURE 5 | Diet-dependent specific correlation between mouse phenotypes and gut microbiota. Spearman's correlation analysis ($|R| \geq 0.5$) between the top 30 abundance genera and metabolic disorder traits (including liver weight, WAT weight, BAT weight, serum HDL, serum LDL, serum TC, serum TG, serum NEFA, liver TG, serum ALT, fasting glucose, and fasting insulin) among three groups, by a pairwise comparisons, including HSD vs. Con (A), HFD vs. Con (B), and HFD vs. HSD (C). $**p < 0.01$, $***p < 0.001$. (D) Mean abundance variation and statistical results of several high phenotypic correlations genus among groups at all-time points. Black circle represents $p < 0.05$.

liver weight, and BAT weight among R-HFD, R-HSD, and Con mice (Figures 6B,C), R-HSD and R-HFD mice showed similar increase in serum TC, and hepatic TG and TC levels

(Figures 6D–G). However, higher increase in WAT weight was observed in R-HFD mice than R-HSD group, while serum LDL levels were higher in R-HSD mice (Figures 6C,E),



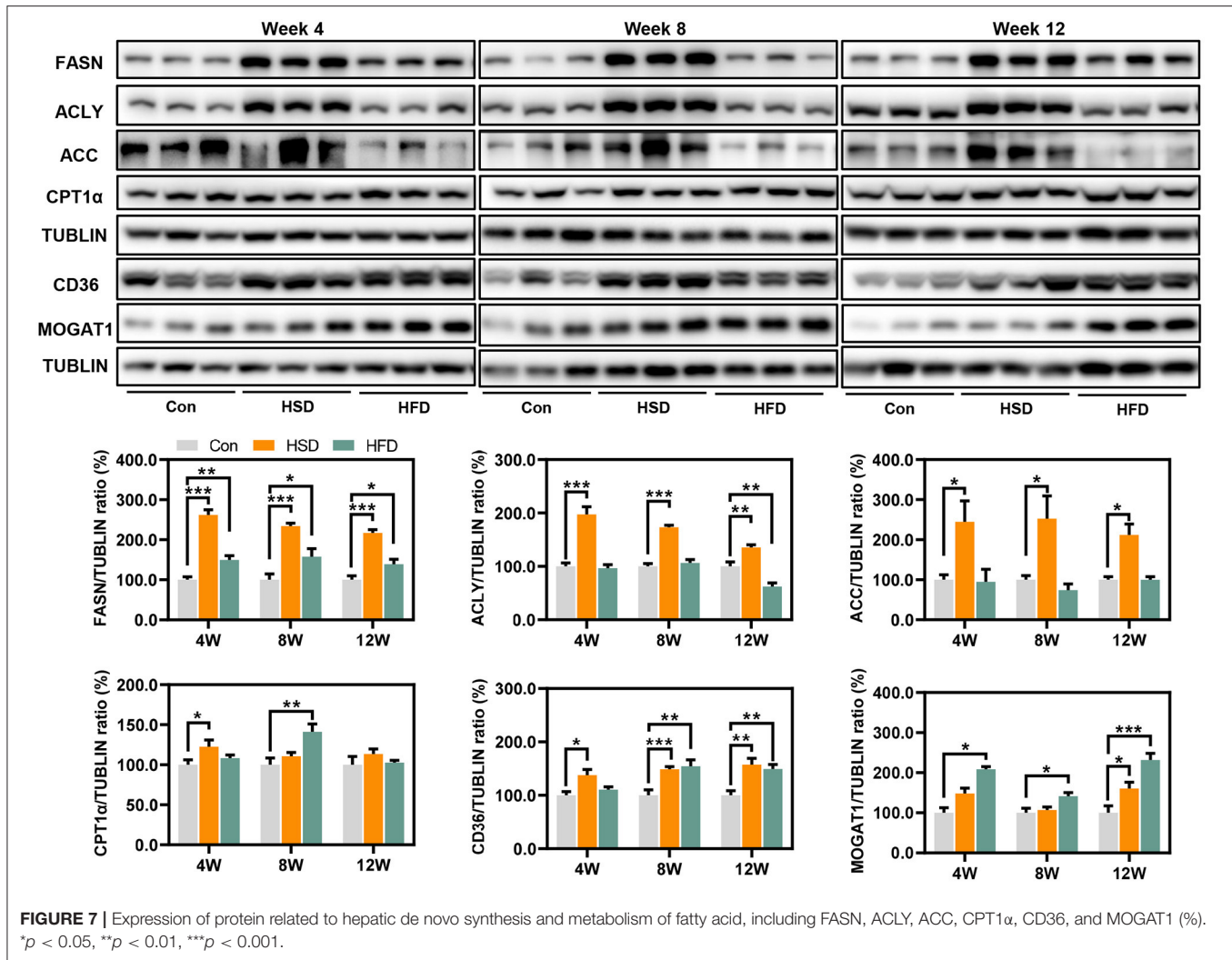
implying that gut microbiota from HFD or HSD mice induced different impacts on recipient mice. These results suggested that the metabolic influence of HSD and HFD is different, and transferable via gut microbiota at certain extent, highlighting the different contributions to metabolic phenotypes of diet-changed gut microbiota in regulating host metabolism.

High-Fat Diet and High-Sucrose Intake Differently Altered the Hepatic Transcriptomic Profile

To explore the regulation of hepatic lipid metabolism under different energy intake conditions, we tested the expression of protein related to hepatic *de novo* synthesis and metabolism of fatty acid. The result showed that HSD can significantly activate the *de novo* synthesis of endogenous fatty acids [fatty

acid synthase (FASN), ATP citrate lyase (ACLY), and acetyl-CoA carboxylase (ACC)] in the liver, although hepatic steatosis was not severe (Figure 7). HSD and HFD could slightly increase the expression of CPT1 α , the rate-limiting enzyme for fatty acid β oxidation, at early stage. Meanwhile, HSD and HFD differently upregulated the protein level of fatty acid transporter CD36 and monoacylglycerol acyltransferase (MOGAT1), leading to the increased accumulation of lipid in the liver (Figure 7).

To explore the effect of different types of energy intake on liver function, we studied hepatic transcriptome in HFD- and HSD-fed mice after 12-week intervention. First, the principal component analysis (PCA) and sample similarity tree showed a distinct separation on the gene expression profiles of 3 groups (Figure 8A). A total of 166 or 322 differentially expressed genes were determined between Con and HSD and between Con and HFD groups, respectively, with the double criteria of both fold



change ≥ 2 (or ≤ 0.5) and $p < 0.05$ (Figure 8B). Interestingly, all 76 common differential genes were observed exactly the same trend in HSD and HFD groups compared with Con group (Figure 8B). We then performed KEGG pathway enrichment analysis on two clusters of differential genes (166 and 322), respectively, using the DAVID Bioinformatics Database (<http://david.abcc.ncifcrf.gov/>). The results showed that HFD and HSD both significantly altered the metabolic pathway, including lipid metabolism (arachidonic acid metabolism; steroid hormone biosynthesis) and retinol metabolism, along with PPAR signaling pathway in endocrine system (Figures 8C,D). HSD significantly altered the genes mainly related to energy metabolism (nitrogen metabolism), bile acid metabolism (primary bile acid biosynthesis; bile secretion), and amino acid metabolism (glycine, serine, and threonine metabolism; alanine, aspartate, and glutamate metabolism) (Figure 8C). Meanwhile, HFD significantly altered the genes related to ovarian steroidogenesis in endocrine system, lipid metabolism (linoleic acid metabolism; biosynthesis of unsaturated fatty acids; fatty acid degradation), and inflammation (inflammatory mediator regulation of TRP

channels) (Figure 8D). Heatmap of enriched genes also showed that HFD significantly reduced fatty acid degradation and increased proinflammatory cytokine, while HSD significantly increased hepatic *de novo* lipogenesis and reduced primary bile acid synthesis alternative pathway (Figure 8E).

In summary, different high-energy dietary types have divergent effect on regulating hepatic gene expression. HSD could promote the *de novo* synthesis of fatty acids and reduce primary bile acid synthesis via the alternative pathway in the liver, while HFD intake mainly inhibits the degradation of fatty acids and activates the inflammatory expression in the liver, leading to a severe hepatic lipid accumulation in general.

DISCUSSION

Metabolic syndrome (MetS) is considered as a pathological state, in which the metabolism of the proteins, fats, carbohydrates, and other substances is disturbed, accompanying a group of complex metabolic disorder syndromes including obesity,

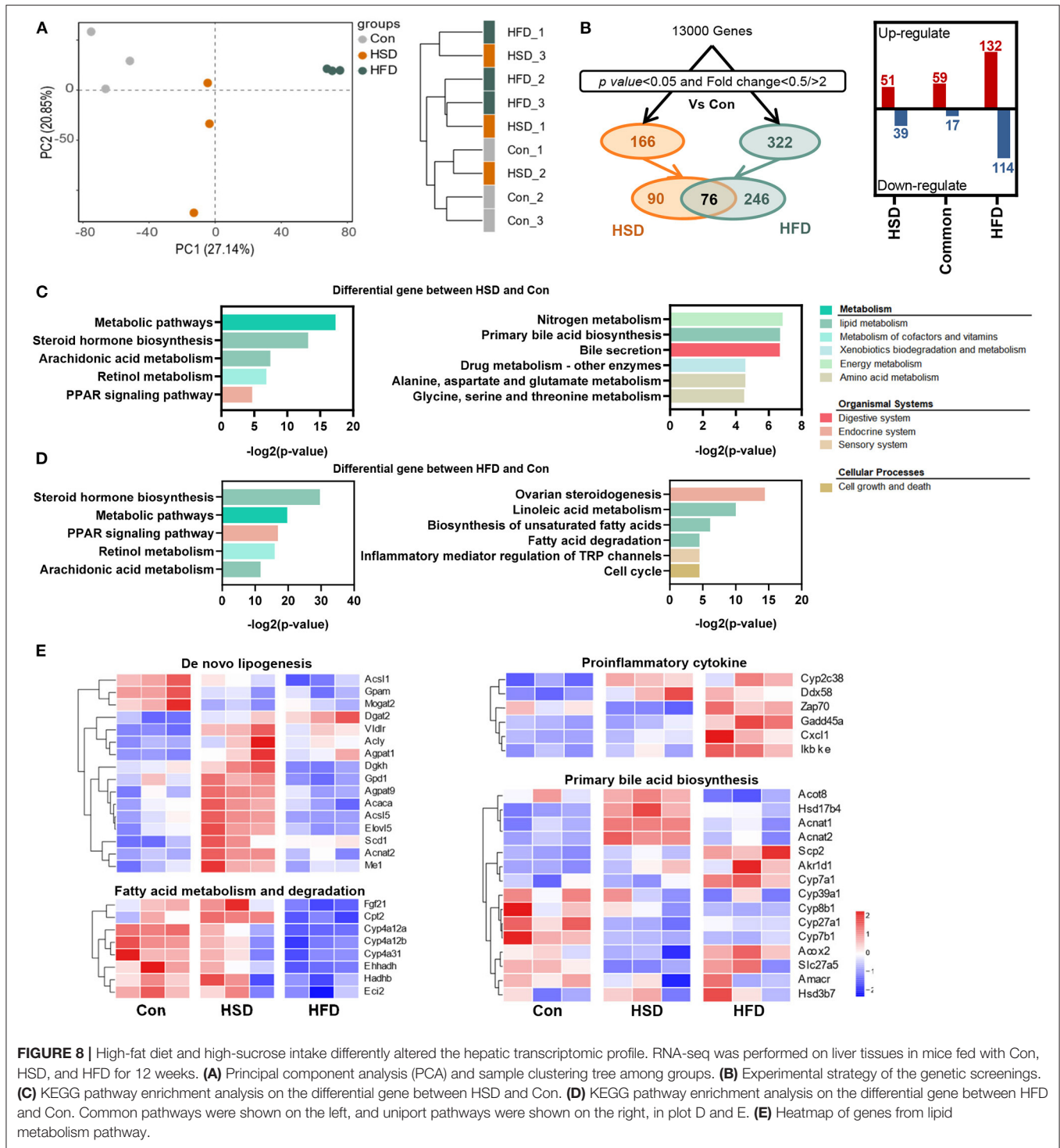


FIGURE 8 | High-fat diet and high-sucrose intake differently altered the hepatic transcriptomic profile. RNA-seq was performed on liver tissues in mice fed with Con, HSD, and HFD for 12 weeks. **(A)** Principal component analysis (PCA) and sample clustering tree among groups. **(B)** Experimental strategy of the genetic screenings. **(C)** KEGG pathway enrichment analysis on the differential gene between HSD and Con. **(D)** KEGG pathway enrichment analysis on the differential gene between HFD and Con. Common pathways were shown on the left, and uniprot pathways were shown on the right, in plot D and E. **(E)** Heatmap of genes from lipid metabolism pathway.

hyperlipidemia, hypercholesterolemia, diabetes, and NAFLD (52–54). Increasing evidence showed the significant impact of high-fat and high-sugar diet on the occurrence and development of metabolic syndrome (55, 56). However, very few studies have compared the similarities and differences of metabolic disorders induced by excessive fat and sugar intake, and how different

high-energy diet-induced divergent gut microbiota composition and function lead to MetS is still unclear.

In this study, we found that both lipid intake and sugar (sucrose) supplementation were sufficient to induce a pronounced obese phenotype and fatty liver in mice during the 12-week experiment with different extends. Increased visceral

fat mass is intimately linked to various metabolic risks. The sharp increase in WAT weight is strongly related to metabolic diseases. Our data showed that HFD induced a fast increase in WAT accumulation at early stage, while HSD played a more persistent effect on increasing WAT during 12-week intervention with higher WAT index in HSD group than HFD group. Interestingly, HSD feeding caused a more significant increase in BAT index, but the increased BAT contains enlarged lipid droplets with pronounced white lipidation, which ultimately leads to mitochondrial dysfunction in BAT (57). We found that 12 weeks of HSD intervention produced hyperlipidemia, manifested by accumulation of serum TG and NEFA, which might be related to the persistent increase in visceral fat weight caused by HSD. Sucrose could be broken into glucose and fructose. On the one hand, glucose could provide a carbon scaffold to promote *de novo* lipogenesis (DNL), which is consistent with the increased expression of DNL-related gene as revealed by our transcriptomic analysis. On the other hand, fructose could turn on the transcriptional program of DNL in the liver and could be metabolized to acetyl-CoA by gut microbiota. In addition, fructose can cause a decrease in lipoprotein lipase, which in turn reduces VLDL level and the clearance of TG-rich lipoproteins, eventually leads to elevated serum TG and NAFA, inducing severe hyperlipidemia (58, 59). In contrast, HFD-induced hypercholesterolemia, impaired glucose tolerance, insulin resistance (IR), and hepatic lipid accumulation were more severe than HSD. Excess dietary fatty acids were taken up by the liver and aggravate liver lipid deposition (60), and ectopic lipid deposition could significantly impair liver function and cause disrupted metabolism of fatty acids. Insulin resistance leads to inappropriate release of fatty acids through dysregulated lipolysis, which further leads to impaired systemic insulin signaling (61), suggesting that HFD-induced lipotoxicity had a greater effect on insulin signaling than sucrose. Meanwhile, liver is the most important organ for cholesterol metabolism. Excessive hepatic cholesterol was transported into the blood through VLDL secretion, resulting in elevated LDL and hypercholesterolemia (62). These findings demonstrate that HFD could induce more severe metabolic disorder than HSD.

In the last two decades, gut microbiota has become an important regulator of host energy metabolism, which is closely related to obesity, NAFLD, and IR (51, 63, 64). Based on 16S rRNA gene sequencing, we found that HFD played a dramatic impact on the structure and function of the gut microbiota throughout the 12-week study. These impacts included significant downregulation of species richness, distinct bacterial community structure from Con group, significant increase in F/B ratio, and dramatic changes in microbial function. We also found that HFD intervention significantly inhibited bacterial glycometabolic-related metabolism pathways and lipid metabolism but activated inflammation signaling. In contrast, there was no significant effect on the overall microbiota structure between HSD and Con group. But after 4-week intervention, the HSD had a significant effect on microbial function such as activation of glycometabolic-related metabolism pathways and inhibition of glycometabolic-related signaling pathway, although the effect was not persistent. Notably, the biosynthesis of primary

and secondary bile acids was significantly activated at 12 weeks of HSD intervention, which is consistent with the hepatic transcriptomic results. The above results suggested that the effect of diet on gut microbiota composition and function is time-dependent, and HFD played a more robust and sustained role in regulation gut microbiota than HSD.

The alteration of gut microbiota induced by diet is thought to be closely related to metabolic phenotype (65). Thus, we first analyzed the correlation between mouse phenotype and bacterial family shifted by HSD or HFD, individually. When analyzing HSD vs. Con groups, since HSD induced less bacterial changes, only *Odoribacter* and *Coprococcus_1* were positively correlated, while *Prevotellaceae_NK3B31_group* was negatively associated, with several metabolic indicators. The Spearman correlation based on HFD vs. Con groups showed two separated clusters. Genera elevated by HFD were associated with most mouse phenotypes, and vice versa. *Odoribacter*, the abundance of which was elevated by HFD and late stage of HSD, also showed positive with WAT weight as well as serum and hepatic lipids when comparing HFD vs. Con, but to a less extent when comparing HFD vs. HSD. However, previous studies found *Odoribacter_splanchnicus*, a butyric acid-producing bacterium, has a negative correlation with adiposity in pterostilbene-treated Zucker (*fa/fa*) rats (66). In addition, *O. splanchnicus* has been associated with a healthy fasting serum lipid profile in postmenopausal women with obesity (67). The inconsistent findings might be due to the different diet intakes as a standard-chow diet and pterostilbene intervention was used in the rat experiment. Moreover, *Norank_f_Bacteroidales_S24-7_group* and *[Eubacterium]_coprostanoligenes_group*, the abundance of which were reduced by HFD and also showed significant difference between HFD and HSD, showed inverse correlation with mouse metabolic indicators when comparing HFD with Con and HFD with HSD, but not when comparing HSD with Con. This finding indicated that these two genera might account for HFD-induced more severe metabolic disorders than HSD. In addition, based on the different reports of gut microbiota composition after HFD feeding (30–32), the different findings of gut microbiota changes might be due to different mouse model, age, HFD used, and sequencing depth. In addition, metabolomics study might be also important to investigate the potential metabolites that participate in host metabolic regulation. Moreover, the FMT results indicated that phenotypic changes after HFD and HSD feeding were due to the alteration of gut microbiota structure and function to a certain extent. Since the colonization or gut microbiota profile in the recipient mice was not analyzed in this study, the direct relationship between certain bacteria and phenotypes needs to be further investigated.

To further study the mechanism of how the two-kind high-energy diet induce specific host metabolism, we carried out hepatic transcriptomic analysis. As observed, HFD altered more gene changes in numbers. Both HSD and HFD could regulate the pathway of PPAR signaling pathway, retinol metabolism, arachidonic acid metabolism, and steroid hormone biosynthesis. These metabolic pathways have been found to be closely related to metabolic disorders in body: Diabetic patients were frequently accompanied by severe imbalances in vitamin A levels (68);

arachidonic acid, as a precursor of various lipid mediators, is involved in inflammatory responses and immune system (69); PPAR signaling pathway had been close related to lipid synthesis and metabolism (70). In addition, HSD significantly inhibits amino acid metabolism pathway and primary bile acid synthesis in alternative pathway. Alanine, serine, threonine, and glycine could generate acetyl coenzyme through pyruvate and then contribute the tricarboxylic acid cycle. The inhibition of their metabolic pathways might be due to the excessive accumulation of acetyl coenzyme A in the liver caused by overdose sugar intake. The alternative pathway for primary bile acid synthesis mainly produced non-12 α -hydroxy bile acids. This study suggested that the activation of the alternative pathway can produce beneficial hydroxylated sterols and detoxify harmful hydroxylated sterols, thereby improving metabolic homeostasis (71, 72). Recently, Todoric et al. (73) stated that excessive intake of fructose would cause hepatic *de novo* lipogenesis. Consistently, after 12 weeks HSD intervention, several important enzymes were significantly upregulated in hepatic for *de novo* fatty acid synthesis, which are more remarkable than HFD. Our results supported that the harmful effect of HSD might be based on the increase in hepatic *de novo* lipogenesis and inhibition of the alternative pathway for primary bile acid synthesis. In contrast, HFD showed significant reduction in fatty acid degradation and increase inflammatory mediator regulation of TRP channels. The widely accepted classical pathogenesis of NAFLD is the “two hit theory,” including the accumulation of lipids in liver cells (the first hit) and inflammatory response triggered by a series of cytotoxic events (the second hit) (74). Triggering of hepatocyte inflammation might be an important reason why HFD produces more severe hepatic metabolic disturbances than HSD.

In conclusion, our results showed that different types of energy intake might have divergent effects on gut microbiota and host metabolism. HSD time-dependently induced metabolic disorder with more severe hypercholesterolemia which might be based on the increase hepatic *de novo* lipogenesis of fatty acid and alternative pathway of bile acid synthesis. In contrast, HFD induced more serious metabolic disorder including obesity, IR, and hepatic lipid accumulation, which might be based on the reduction in fatty acid degradation and increase inflammation.

REFERENCES

- Eckel RH, Grundy SM, Zimmet PZ. The metabolic syndrome. *Lancet*. (2005) 365:1415–28. doi: 10.1016/S0140-6736(05)66378-7
- Kassi E, Pervanidou P, Kaltsas G, Chrousos G. Metabolic syndrome: definitions and controversies. *BMC Med*. (2011) 9:48. doi: 10.1186/1741-7015-9-48
- Després JP, Lemieux I. Abdominal obesity and metabolic syndrome. *Nature*. (2006) 444:881–7. doi: 10.1038/nature05488
- Wainwright P, Byrne CD. Bidirectional relationships and disconnects between NAFLD and features of the metabolic syndrome. *Int J Mol Sci*. (2016) 17:367. doi: 10.3390/ijms17030367
- Yki-Järvinen H. Non-alcoholic fatty liver disease as a cause and a consequence of metabolic syndrome. *Lancet Diabetes Endocrinol*. (2014) 2:901–10. doi: 10.1016/S2213-8587(14)70032-4

Meanwhile, HFD played a more robust and sustained role than HSD in regulating the structure and function of gut microbiota, and the metabolic detrimental effects can be transferred through fecal microbiota transplantation, suggesting both diet and diet-induced gut microbiota alteration may account for the divergent dietary effect on host metabolism.

DATA AVAILABILITY STATEMENT

The data presented in the study are deposited in the Data Availability Statement repository, accession number for Transcriptomics Array: GSE206601, GSM6257592, GSM6257593, GSM6257594, GSM6257595, GSM6257596, GSM6257597, GSM6257598, GSM6257599, GSM6257600, for 16S rRNA Gene Sequencing: SRP379710 (PRJNA848196).

ETHICS STATEMENT

The animal study was reviewed and approved by Animal Experiment Institution of Shanghai University of Traditional Chinese Medicine.

AUTHOR CONTRIBUTIONS

WZ and YH conducted the FMT animal experiments and data analysis. YuL conducted the time-course animal experiment. YaL, JZ, and XH helped in animal experiments. NZ helped in data analysis. LS designed and revised the manuscript. HL conceptualized and supervised the whole study and revised the manuscript.

FUNDING

This work was supported by the Joint Funds of the National Natural Science Foundation of China (No. U21A20413), the National Natural Science Foundation of China (No. 81873059 and 82004016), the National Science Foundation of Shanghai (No. 20ZR1453900), Shanghai Excellent Academic Leaders Program (No. 21XD1403500), and Shanghai Pujiang Program (No. 20PJ1413100).

- Mozzak M, Szulińska M, Bogdański P. You are what you eat—the relationship between diet, microbiota, and metabolic disorders—a review. *Nutrients*. (2012) 12:1096. doi: 10.3390/nu12041096
- Harrison S, Couture P, Lamarche B. Diet quality, saturated fat and metabolic syndrome. *Nutrients*. (2020) 12:3232. doi: 10.3390/nu12113232
- Zinöcker MK, Lindseth IA. The western diet-microbiome-host interaction and its role in metabolic disease. *Nutrients*. (2018) 10:365. doi: 10.3390/nu10030365
- Martinez KB, Leone V, Chang EB. Western diets, gut dysbiosis, and metabolic diseases: are they linked? *Gut Microbes*. (2017) 8:130–42. doi: 10.1080/19490976.2016.1270811
- Kuziel GA, Rakoff-Nahoum S. The gut microbiome. *Curr Biol*. (2022) 32:R257–r264. doi: 10.1016/j.cub.2022.02.023

11. Kolodziejczyk AA, Zheng D, Elinav E. Diet-microbiota interactions and personalized nutrition. *Nat Rev Microbiol.* (2019) 17:742–53. doi: 10.1038/s41579-019-0256-8
12. Krajmalnik-Brown R, Ilhan ZE, Kang DW, DiBaise JK. Effects of gut microbes on nutrient absorption and energy regulation. *Nutr Clin Pract.* (2012) 27:201–14. doi: 10.1177/0884533611436116
13. Krautkramer KA, Fan J, Bäckhed F. Gut microbial metabolites as multi-kingdom intermediates. *Nat Rev Microbiol.* (2021) 19:77–94. doi: 10.1038/s41579-020-0438-4
14. Wu J, Wang K, Wang X, Pang Y, Jiang C. The role of the gut microbiome and its metabolites in metabolic diseases. *Protein Cell.* (2021) 12:360–73. doi: 10.1007/s13238-020-00814-7
15. Sanna S, van Zuydam NR, Mahajan A, Kurilshikov A, Vich Vila A, Vösa U, et al. Causal relationships among the gut microbiome, short-chain fatty acids and metabolic diseases. *Nat Genet.* (2019) 51:600–5. doi: 10.1038/s41588-019-0350-x
16. Yoon HS, Cho CH, Yun MS, Jang SJ, You HJ, Kim JH, et al. Akkermansia muciniphila secretes a glucagon-like peptide-1-inducing protein that improves glucose homeostasis and ameliorates metabolic disease in mice. *Nat Microbiol.* (2021) 6:563–73. doi: 10.1038/s41564-021-00880-5
17. Fuke N, Nagata N, Suganuma H, Ota T. Regulation of Gut Microbiota and Metabolic Endotoxemia with Dietary Factors. *Nutrients.* (2019) 11:2277. doi: 10.3390/nu11102277
18. Guerville M, Leroy A, Siquin A, Laugerette F, Michalski MC, Boudry G. Western-diet consumption induces alteration of barrier function mechanisms in the ileum that correlates with metabolic endotoxemia in rats. *Am J Physiol Endocrinol Metab.* (2017) 313:E107–e120. doi: 10.1152/ajpendo.00372.2016
19. Cani PD, Amar J, Iglesias MA, Poggi M, Knauf C, Bastelica D, et al. Metabolic endotoxemia initiates obesity and insulin resistance. *Diabetes.* (2007) 56:1761–72. doi: 10.2337/db06-1491
20. Cani PD, Bibiloni R, Knauf C, Waget A, Neyrinck AM, Delzenne NM, et al. Changes in gut microbiota control metabolic endotoxemia-induced inflammation in high-fat diet-induced obesity and diabetes in mice. *Diabetes.* (2008) 57:1470–81. doi: 10.2337/db07-1403
21. Serino M, Luche E, Gres S, Baylac A, Bergé M, Cenac C, et al. Metabolic adaptation to a high-fat diet is associated with a change in the gut microbiota. *Gut.* (2012) 61:543–53. doi: 10.1136/gutjnl-2011-301012
22. Fan Y, Pedersen O. Gut microbiota in human metabolic health and disease. *Nat Rev Microbiol.* (2021) 19:55–71. doi: 10.1038/s41579-020-0433-9
23. Bouter KE, van Raalte DH, Groen AK, Nieuwdorp M. Role of the gut microbiome in the pathogenesis of obesity and obesity-related metabolic dysfunction. *Gastroenterology.* (2017) 152:1671–8. doi: 10.1053/j.gastro.2016.12.048
24. Moreno-Fernández S, Garcés-Rimón M, Vera G, Astier J, Landrier JF, Miguel M. High Fat/High Glucose Diet Induces Metabolic Syndrome in an Experimental Rat Model. *Nutrients.* (2018) 10:1502. doi: 10.3390/nu10101502
25. Melo BF, Sacramento JF, Ribeiro MJ, Prego CS, Correia MC, Coelho JC, et al. Evaluating the impact of different hypercaloric diets on weight gain, insulin resistance, glucose intolerance, and its comorbidities in rats. *Nutrients.* (2019) 11:1197. doi: 10.3390/nu11061197
26. Buettner R, Schölmerich J, Bollheimer LC. High-fat diets: modeling the metabolic disorders of human obesity in rodents. *Obesity.* (2007) 15:798–808. doi: 10.1038/oby.2007.608
27. Leonardi BF, Gosmann G, Zimmer AR. Modeling diet-induced metabolic syndrome in rodents. *Mol Nutr Food Res.* (2020) 64:e2000249. doi: 10.1002/mnfr.202000249
28. Turnbaugh PJ, Ridaura VK, Faith JJ, Rey FE, Knight R, Gordon JJ. The effect of diet on the human gut microbiome: a metagenomic analysis in humanized gnotobiotic mice. *Sci Transl Med.* (2009) 1:6ra14. doi: 10.1126/scitranslmed.3000322
29. Wan Y, Wang F, Yuan J, Li J, Jiang D, Zhang J, et al. Effects of dietary fat on gut microbiota and faecal metabolites, and their relationship with cardiometabolic risk factors: a 6-month randomised controlled-feeding trial. *Gut.* (2019) 68:1417–29. doi: 10.1136/gutjnl-2018-317609
30. Yang J, Wei H, Zhou Y, Szeto CH, Li C, Lin Y, et al. High-fat diet promotes colorectal tumorigenesis through modulating gut microbiota and metabolites. *Gastroenterology.* (2022) 162:135–49.e132. doi: 10.1053/j.gastro.2021.08.041
31. Wang P, Gao J, Ke W, Wang J, Li D, Liu R, et al. Resveratrol reduces obesity in high-fat diet-fed mice via modulating the composition and metabolic function of the gut microbiota. *Free Radic Biol Med.* (2020) 156:83–98. doi: 10.1016/j.freeradbiomed.2020.04.013
32. Hong Y, Sheng L, Zhong J, Tao X, Zhu W, Ma J, et al. Desulfovibrio vulgaris, a potent acetic acid-producing bacterium, attenuates nonalcoholic fatty liver disease in mice. *Gut Microbes.* (2021) 13:1–20. doi: 10.1080/19490976.2021.1930874
33. Do MH, Lee E, Oh MJ, Kim Y, Park HY. High-glucose or -fructose diet cause changes of the gut microbiota and metabolic disorders in mice without body weight change. *Nutrients.* (2018) 10:761. doi: 10.3390/nu10060761
34. Voreades N, Kozil A, Weir TL. Diet and the development of the human intestinal microbiome. *Front Microbiol.* (2014) 5:494. doi: 10.3389/fmicb.2014.00494
35. Zmora N, Suez J, Elinav E. You are what you eat: diet, health and the gut microbiota. *Nat Rev Gastroenterol Hepatol.* (2019) 16:35–56. doi: 10.1038/s41575-018-0061-2
36. Beam A, Clinger E, Hao L. Effect of diet and dietary components on the composition of the gut microbiota. *Nutrients.* (2021) 13:2795. doi: 10.3390/nu13082795
37. Kleiner DE, Brunt EM, Van Natta M, Behling C, Contos MJ, Cummings OW, et al. Design and validation of a histological scoring system for nonalcoholic fatty liver disease. *Hepatology.* (2005) 41:1313–21. doi: 10.1002/hep.20701
38. Folch J, Lees M, Sloane Stanley GH. A simple method for the isolation and purification of total lipides from animal tissues. *J Biol Chem.* (1957) 226:497–509. doi: 10.1016/S0021-9258(18)64849-5
39. Sinha R, Abu-Ali G, Vogtmann E, Fodor AA, Ren B, Amir A, et al. Assessment of variation in microbial community amplicon sequencing by the microbiome quality control (MBQC) project consortium. *Nat Biotechnol.* (2017) 35:1077–86. doi: 10.1038/nbt.3981
40. Chen S, Zhou Y, Chen Y, Gu J. fastp: an ultra-fast all-in-one FASTQ preprocessor. *Bioinformatics.* (2018) 34:i884–90. doi: 10.1093/bioinformatics/bty560
41. Magoc T, Salzberg SL. FLASH: fast length adjustment of short reads to improve genome assemblies. *Bioinformatics.* (2011) 27:2957–63. doi: 10.1093/bioinformatics/btr507
42. Edgar RC. UPARSE: highly accurate OTU sequences from microbial amplicon reads. *Nat Methods.* (2013) 10:996–8. doi: 10.1038/nmeth.2604
43. Edgar RC, Haas BJ, Clemente JC, Quince C, Knight R. UCHIME improves sensitivity and speed of chimera detection. *Bioinformatics.* (2011) 27:2194–200. doi: 10.1093/bioinformatics/btr381
44. Quast C, Pruesse E, Yilmaz P, Gerken J, Schweer T, Yarza P, et al. ribosomal RNA gene database project: improved data processing and web-based tools. *Nucleic Acids Res.* (2013) 41:D590–596. doi: 10.1093/nar/gks1219
45. Wang Q, Garrity GM, Tiedje JM, Cole JR. Naive bayesian classifier for rapid assignment of rRNA sequences into the new bacterial taxonomy. *Appl Environ Microbiol.* (2007) 73:5261–7. doi: 10.1128/AEM.00062-07
46. Schloss PD, Westcott SL, Ryabin T, Hall JR, Hartmann M, Hollister EB, et al. Introducing mothur: open-source, platform-independent, community-supported software for describing and comparing microbial communities. *Appl Environ Microbiol.* (2009) 75:7537–41. doi: 10.1128/AEM.01541-09
47. Lozupone C, Lladser ME, Knights D, Stombaugh J, Knight R. UniFrac: an effective distance metric for microbial community comparison. *ISME J.* (2011) 5:169–72. doi: 10.1038/ismej.2010.133
48. Caporaso JG, Kuczynski J, Stombaugh J, Bittinger K, Bushman FD, Costello EK, et al. QIIME allows analysis of high-throughput community sequencing data. *Nat Methods.* (2010) 7:335–6. doi: 10.1038/nmeth.f.303
49. Langille MG, Zaneveld J, Caporaso JG, McDonald D, Knights D, Reyes JA, et al. Predictive functional profiling of microbial communities using 16S rRNA marker gene sequences. *Nat Biotechnol.* (2013) 31:814–21. doi: 10.1038/nbt.2676
50. Canfora EE, Meex RCR, Venema K, Blaak EE. Gut microbial metabolites in obesity, NAFLD and T2DM. *Nat Rev Endocrinol.* (2019) 15:261–73. doi: 10.1038/s41574-019-0156-z
51. Leung C, Rivera L, Furness JB, Angus PW. The role of the gut microbiota in NAFLD. *Nat Rev Gastroenterol Hepatol.* (2016) 13:412–25. doi: 10.1038/nrgastro.2016.85

52. Scherer T, Sakamoto K, Buettner C. Brain insulin signalling in metabolic homeostasis and disease. *Nat Rev Endocrinol.* (2021) 17:468–83. doi: 10.1038/s41574-021-00498-x
53. Powell EE, Wong VW, Rinella M. Non-alcoholic fatty liver disease. *Lancet.* (2021) 397:2212–24. doi: 10.1016/S0140-6736(20)32511-3
54. Czech MP. Insulin action and resistance in obesity and type 2 diabetes. *Nat Med.* (2017) 23:804–14. doi: 10.1038/nm.4350
55. Ludwig DS, Willett WC, Volek JS, Neuhouser ML. Dietary fat: From foe to friend? *Science.* (2018) 362:764–70. doi: 10.1126/science.aau2096
56. Ludwig DS, Hu FB, Tappy L, Brand-Miller J. Dietary carbohydrates: role of quality and quantity in chronic disease. *BMJ.* (2018) 361:k2340. doi: 10.1136/bmj.k2340
57. Shimizu I, Aprahamian T, Kikuchi R, Shimizu A, Papanicolaou KN, MacLaughlan S, et al. Vascular rarefaction mediates whitening of brown fat in obesity. *J Clin Invest.* (2014) 124:2099–112. doi: 10.1172/JCI71643
58. Morigny P, Boucher J, Arner P, Langin D. Lipid and glucose metabolism in white adipocytes: pathways, dysfunction and therapeutics. *Nat Rev Endocrinol.* (2021) 17:276–95. doi: 10.1038/s41574-021-00471-8
59. Zhao S, Jang C, Liu J, Uehara K, Gilbert M, Izzo L, et al. Dietary fructose feeds hepatic lipogenesis via microbiota-derived acetate. *Nature.* (2020) 579:586–91. doi: 10.1038/s41586-020-2101-7
60. Park JG, Xu X, Cho S, Hur KY, Lee MS, Kersten S, et al. CREBH-FGF21 axis improves hepatic steatosis by suppressing adipose tissue lipolysis. *Sci Rep.* (2016) 6:27938. doi: 10.1038/srep27938
61. Perry RJ, Camporez JG, Kursawe R, Titchenell PM, Zhang D, Perry CJ, et al. Hepatic acetyl CoA links adipose tissue inflammation to hepatic insulin resistance and type 2 diabetes. *Cell.* (2015) 160:745–58. doi: 10.1016/j.cell.2015.01.012
62. Luo J, Yang H, Song BL. Mechanisms and regulation of cholesterol homeostasis. *Nat Rev Mol Cell Biol.* (2020) 21:225–45. doi: 10.1038/s41580-019-0190-7
63. Le Chatelier E, Nielsen T, Qin JJ, Prifti E, Hildebrand F, Falony G, et al. Richness of human gut microbiome correlates with metabolic markers. *Nature.* (2013) 500:541–6. doi: 10.1038/nature12506
64. Dao MC, Everard A, Aron-Wisniewsky J, Sokolovska N, Prifti E, Verger EO, et al. Akkermansia muciniphila and improved metabolic health during a dietary intervention in obesity: relationship with gut microbiome richness and ecology. *Gut.* (2016) 65:426–36. doi: 10.1136/gutjnl-2014-308778
65. Kong C, Gao R, Yan X, Huang L, Qin H. Probiotics improve gut microbiota dysbiosis in obese mice fed a high-fat or high-sucrose diet. *Nutrition.* (2019) 60:175–84. doi: 10.1016/j.nut.2018.10.002
66. Etxeberria U, Hijona E, Aguirre L, Milagro FI, Bujanda L, Rimando AM, et al. Pterostilbene-induced changes in gut microbiota composition in relation to obesity. *Mol Nutr Food Res.* (2017) 61. doi: 10.1002/mnfr.201500906
67. Brahe LK, Le Chatelier E, Prifti E, Pons N, Kennedy S, Hansen T, et al. Specific gut microbiota features and metabolic markers in postmenopausal women with obesity. *Nutr Diabetes.* (2015) 5:e159. doi: 10.1038/nutd.2015.9
68. Iqbal S, Naseem I. Role of vitamin A in type 2 diabetes mellitus biology: effects of intervention therapy in a deficient state. *Nutrition.* (2015) 31:901–7. doi: 10.1016/j.nut.2014.12.014
69. Das UN. Essential Fatty Acids and Their Metabolites in the Pathobiology of Inflammation and Its Resolution. *Biomolecules.* (2021) 11. doi: 10.3390/biom11121873
70. Gross B, Pawlak M, Lefebvre P, Staels B. PPARs in obesity-induced T2DM, dyslipidaemia and NAFLD. *Nat Rev Endocrinol.* (2017) 13:36–49. doi: 10.1038/nrendo.2016.135
71. Zheng X, Chen T, Jiang R, Zhao A, Wu Q, Kuang J, et al. Hyocholic acid species improve glucose homeostasis through a distinct TGR5 and FXR signaling mechanism. *Cell Metab.* (2021) 33:791–803. e797. doi: 10.1016/j.cmet.2020.11.017
72. Jia W, Xie G, Jia W. Bile acid-microbiota crosstalk in gastrointestinal inflammation and carcinogenesis. *Nat Rev Gastroenterol Hepatol.* (2018) 15:111–28. doi: 10.1038/nrgastro.2017.119
73. Todoric J, Di Caro G, Reibe S, Henstridge DC, Green CR, Vrbanc A, et al. Fructose stimulated de novo lipogenesis is promoted by inflammation. *Nat Metab.* (2020) 2:1034–45. doi: 10.1038/s42255-020-0261-2
74. Day CP, James OF. Steatohepatitis: a tale of two “hits”? *Gastroenterology.* (1998) 114:842–5. doi: 10.1016/S0016-5085(98)70599-2

Conflict of Interest: The authors declare that the research was conducted in the absence of any commercial or financial relationships that could be construed as a potential conflict of interest.

Publisher’s Note: All claims expressed in this article are solely those of the authors and do not necessarily represent those of their affiliated organizations, or those of the publisher, the editors and the reviewers. Any product that may be evaluated in this article, or claim that may be made by its manufacturer, is not guaranteed or endorsed by the publisher.

Copyright © 2022 Zhu, Hong, Li, Li, Zhong, He, Zheng, Sheng and Li. This is an open-access article distributed under the terms of the Creative Commons Attribution License (CC BY). The use, distribution or reproduction in other forums is permitted, provided the original author(s) and the copyright owner(s) are credited and that the original publication in this journal is cited, in accordance with accepted academic practice. No use, distribution or reproduction is permitted which does not comply with these terms.